THE OPTICAL EMISSION FROM A FAST SHOCK WAVE WITH APPLICATION TO SUPERNOVA REMNANTS

ROGER A. CHEVALIER
Kitt Peak National Observatory[1]

ROBERT P. KIRSHNER[2]
University of Michigan

AND

JOHN C. RAYMOND
Harvard-Smithsonian Center for Astrophysics
Received 1979 June 6; accepted 1979 July 12

ABSTRACT

We have observed the spectrum of Tycho's supernova remnant and have detected only the Hα, Hβ, and Hγ lines. The Hα line profile can be divided into two components: one with a width consistent with the instrumental resolution and one with a full width at half-maximum (FWHM) of 1800 $\pm$ 200 km s^{-1}. The two components have similar intensities. The observations are interpreted in terms of a shock wave model. The shock wave is presumably encountering neutral atoms that have some probability of giving line emission before being ionized by the post-shock gas. Charge exchange can occur in the post-shock region, giving rise to a broad emission component from a population of fast neutral atoms. The ratio of broad to narrow emission components is a sensitive function of shock velocity because the charge-exchange cross section depends strongly on the proton velocity. For Tycho's remnant, both the ratio of broad to narrow emission and the FWHM of the broad emission can be fitted if the shock velocity is 2300 $\pm$ 500 km s^{-1}. Combined with the proper motion of the filament as found by Kamper and van den Bergh, the distance to Tycho's remnant is about 2.3 $\pm$ 0.5 kpc. The absolute photographic magnitude of Tycho's supernova at maximum is then -18.8 ± 1.3, which is consistent with the absolute magnitudes of extragalactic Type I supernovae at maximum light.

The shock model can be applied to some other emission nebulae. We predict that a broad emission component should be present in the Hα line profile of the remnant of SN 1006. If the model applies to the high-velocity emission regions in the Cygnus Loop observed by Kirshner and Taylor, we expect the high-velocity components to have a width approximately equal to half their velocity shift and to be unobservable in forbidden emission lines of heavy elements. The model may also apply to the high-velocity emission region observed by Elliott near η Carinae.

Subject headings: nebulae: supernova remnants — shock waves

I. INTRODUCTION

Observations of Tycho's supernova remnant (Kirshner and Chevalier 1978) and the remnant of SN 1006 (Schweizer and Lasker 1978) have shown similar, unusual spectra. Only lines of H have been convincingly detected, and the lines have a substantial narrow component. The emission characteristics can be explained by a model involving the motion of a fast shock wave into a partially neutral medium (Chevalier and Raymond 1978, hereafter CR). Ambient neutral atoms are overrun by the collisionless shock wave and have some probability of emitting line radiation before being ionized. The proper-motion observations of Tycho's remnant (Kamper and van den Bergh 1978) give strong evidence that a fast shock wave is involved.

The theoretical work of CR gave rise to several predictions. One was that lines of He I should be the next brightest optical lines after the Balmer lines. Another was that there should be some fraction of the H emission in a broad component, as a result of charge exchange. In order to test these predictions, we have obtained new observations of Tycho's remnant, which are described in § II. Some new aspects of the theoretical emission model are given in § III. The first part deals with the emission from the broad component in greater detail than was given in CR. The model predictions are then compared to the observations of Tycho's remnant. The third part deals with the case where the gas is optically thick in the lower Lyman lines and gives the resulting Balmer

186

TABLE 1

OBSERVATIONS OF TYCHO KNOT "g"

Variable	1978 August 30 (UT)	1978 August 31 (UT)
Grating	300 mm^{-1}	300 mm^{-1}
Blaze	blue	red
Aperture	5.5" circle	5.5" circle
Integration	4000 s	12,400 s
Wavelengths	3500–7000 Å	4100–7600 Å

decrement. This situation may apply in both Tycho's remnant and the remnant of SN 1006. In § IV, the model is applied to the remnant of SN 1006, the Cygnus Loop, and the high-velocity region near η Carinae. The results are summarized and discussed in § V.

II. OBSERVATIONS OF TYCHO'S SUPERNOVA REMNANT

We observed Tycho's remnant on two nights of excellent seeing and transparency in 1978 August with the image dissector scanner at the Mayall 4 m telescope at KPNO, as detailed in Table 1. We obtained spectra of the knot labeled "g" by Kamper and van den Bergh (1978) which (taking into account its rapid proper motion) was located approximately 214" east and 78" north of the nominal center of the remnant which is at $\alpha = 00^h22^m31^s$, $\delta = +63°51'.6$ (1950.0). This is the brightest and northernmost of the condensations in the eastern filament of the remnant, and it is included in the long-slit observations of Kirshner and Chevalier (1978). The knot is exceedingly faint, so the good sky subtraction that is possible with the image dissector represents a real improvement over the earlier photographic work, in which the sky subtraction is less reliable. Observations of the object and of the sky were made simultaneously through two circular apertures of 5".5 diameter separated by 52" in the focal plane.

The observations were reduced to fluxes through observation of standard stars and the use of Kitt Peak's reduction programs. The lines which are definitely detected are Hα, Hβ, and Hγ. This is consistent with the result of Kirshner and Chevalier who detected only Hα and Hβ, but did not observe in the wavelength range of Hγ. In Table 2, we give our best estimates of the observed line ratios based on both the statistical uncertainty in each measurement and the agreement between our two nights of data. To compare the Balmer line ratios with our models, we need to apply a correction for reddening. There have been several estimates of the reddening to Tycho's supernova based on contemporary observations of the supernova in 1572 (see, e.g., Baade 1945), where it is assumed that its intrinsic colors were those of a Type I extragalactic supernova. In this way, Minkowski (1964) deduced $A_v = 2.1$ and van den Bergh (1970) deduced $A_v = 1.6 \pm 0.1$. However, recent supernova color curves (e.g., Barbon, Ciatti, and Rosino 1973) show that Type I supernovae at maximum are bluer than was assumed by the above authors. Pskovskii (1978) has made a complete reanalysis of the data on Tycho's supernova and has obtained $A_v = 1.92 \pm 0.12$. While Baade (1945) deduced that the supernova maximum occurred on November 15 when $m_v = -4.0 \pm 0.3$, Pskovskii deduces that the maximum occurred on November 5 when $m_v = -4.5 \pm 0.2$. The difference in the day of maximum is important in determining A_v because of the rapid reddening of Type I supernovae near maximum light. With November 15 as the day of maximum, the estimate of A_v increases by more than a magnitude. A distance-dependent determination of A_v can be obtained by examining the absorption toward stars in the direction of Tycho's remnant. Using this method, Brodskaya and Grigor'eva (1962) give A_v as a function of distance modulus. At a distance of 2.3 kpc (see § III), the value of A_v is very uncertain, but may be in the range 2.8 ± 1.0. With these considerations in mind, we have adopted an absorption $A_v = 2.1 \pm 0.5$. In Table 2, we have applied the reddening law derived by Whitford (1958) in the form given by Miller and Mathews (1972). The possible range of $I(\text{H}\alpha)/I(\text{H}\beta)$ is 3.5($A_v = 2.6$) to 5.0($A_v = 1.6$).

TABLE 2

LINE STRENGTHS IN TYCHO'S REMNANT

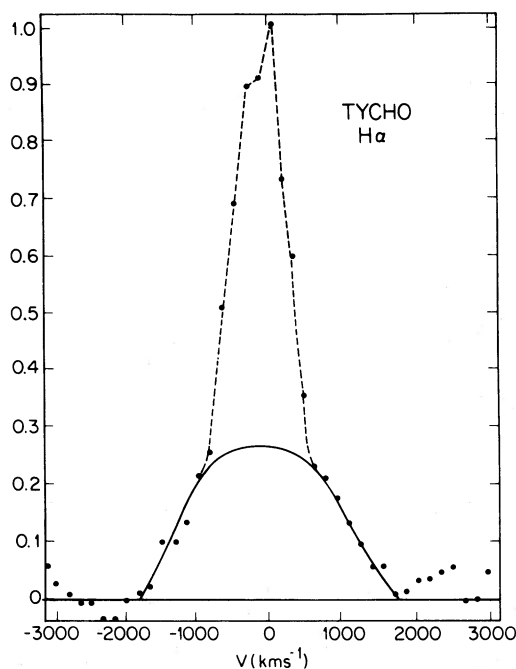| Line	Observed	Intrinsic $(A_v = 2.1)$
Hγ λ4340	22 ± 10	31 ± 14
He II λ4686	< 10	< 11
Hβ λ4861	100	100
He I λ5876	< 7	< 4
Hα λ6562	880 ± 50	410 ± 25
Total Hα flux (ergs cm^{-2} s^{-1})...	$9 \pm 5 \times 10^{-15}$	$40 \pm 25 \times 10^{-15}$

FIG. 1.—The Hα line profile observed in Tycho's supernova remnant as a function of radial velocity; the zero velocity is defined by the rest wavelength of the Hα line. The dots represent the data points actually observed with the Image Dissector Scanner. The dashed line is a fit to the narrow component of the line; its width is consistent with the instrumental resolution. The solid line is a fit to the broad component of the line profile.

The total Hα flux is quite uncertain since the region of emission is comparable in size to the measuring aperture and very faint. A small error in positioning the telescope can produce a substantial change in the measured flux, so that the absolute flux from knot "g" is known only to a factor of 2.

In the photographic work, Kirshner and Chevalier noted that the Hα line might have broad wings. The present image-dissector data in Figure 1 show both a narrow component (which has the same apparent width as night sky lines, and is therefore not resolved) and a broad component which extends in both directions from the narrow component. This broad feature is not present in the spectra of any of the comparison lamps, is not seen in night sky lines, and is not detected in any other object observed with this equipment on any night of our run. The broad feature appears on both nights, is seen for both Hα and Hβ, and agrees with the earlier photographic work: there can be no doubt that it is real.

However, because the instrumental resolution is so coarse (about 20 Å), the decomposition of the line profile into its broad and narrow parts is quite uncertain. The lines sketched in Figure 1 represent a reasonable, but not unique, separation of the Hα profile into two parts. We estimate that the ratio of the broad to narrow components of Hα is in the range 0.4–1.3. Further observations at higher resolution can provide a better estimate of this ratio.

We find that the line profile at Hβ is consistent with the line profile observed at Hα, but at Hγ the data are too noisy to detect any broad component. Both the Hα and Hβ profiles indicate a slight asymmetry, in which the redward wing of the broad component is somewhat more extended than the blue wing. The broad component has an apparent full width at half-maximum (FWHM) of 2000 km s^{-1}; when this is corrected for the instrumental contribution of about 900 km s^{-1}, we find a width of 1800 ± 200 km s^{-1}.

III. THE SHOCK EMISSION MODEL

a) The Broad Component of Emission

Both of our scans of Tycho's remnant show evidence for an emission component with a broad velocity width. The reason for expecting a broad component is that some of the fast protons can undergo charge exchange as mentioned by CR. We now examine this process in more detail.

The important processes for ionizing an incoming neutral particle are ionization by protons and ionization by electrons. This is true unless both the incoming neutral fraction is large and the shock velocity is in a range where charge exchange is the dominant process. Under these circumstances, ionization by neutral atoms can be important. However, here we assume that ionization by neutrals is small and we let σ_i denote the sum of the cross sections for ionization by protons and electrons because the densities of electrons, n_e, and protons, n_p,

are approximately equal. We assume that after a slow neutral atom has been ionized in the post-shock region, the resulting proton and electron are immediately accelerated to high velocity. This can occur through the interaction of the particles with the magnetic field. Under these conditions, the lifetime of a slow neutral particle in the post-shock medium is approximately

$$\tau_s \approx \frac{1}{n_p(\langle \sigma_i v \rangle_s + \langle \sigma_x v \rangle_s)} , \tag{1}$$

where σ_x is the charge-exchange cross section and the angular brackets with subscript s denote an average over the relative velocity, v, between a slow neutral particle and a fast charged particle. The fraction of the incoming neutral particles that undergoes charge exchange is $\langle \sigma_x v \rangle_s / (\langle \sigma_i v \rangle_s + \langle \sigma_x v \rangle_s)$. The interaction results in a fast neutral particle which has a lifetime $(n_p \langle \sigma_i v \rangle_f)^{-1}$, where the angular bracket with subscript f denotes an average over the relative velocity between a fast neutral particle and a fast charged particle. Thus, considering a steady situation, the ratio of the fraction of fast neutral particles, f_f, to the fraction of slow neutral particles, f_s, is

$$\frac{f_f}{f_s} = \left(\frac{\langle \sigma_x v \rangle_s}{(\langle \sigma_i v \rangle_s + \langle \sigma_x v \rangle_s)} \frac{1}{n_p \langle \sigma_i v \rangle_f} \right) \Big/ \left(\frac{1}{n_p(\langle \sigma_i v \rangle_s + \langle \sigma_x v \rangle_s)} \right)$$

$$= \frac{\langle \sigma_x v \rangle_s}{\langle \sigma_i v \rangle_f} . \tag{2}$$

The computation of the average cross sections involves an integral over the velocity distribution. For the charge-exchange cross section, the slow neutral particles can be considered to be stationary so that

$$\langle \sigma_x v \rangle_s = \frac{l^{3/2}}{\pi^{3/2}} \int\int\int_{-\infty}^{+\infty} v\sigma_x(v) \exp \{-l^2[v_x^2 + v_y^2 + (v_z - v_0)^2]\} dv_x dv_y dv_z , \tag{3}$$

where

$$l \equiv \left(\frac{m_p}{2kT} \right)^{1/2} ,$$

m_p is the proton mass, k is Boltzmann's constant, and T is the proton temperature. We have assumed a Cartesian coordinate system in which the z coordinate is perpendicular to the shock front. The velocity v_0 is the bulk velocity of the shocked gas. For a strong adiabatic shock wave in a $\gamma = 5/3$ gas, $v_0 = \frac{3}{4} V_{sh}$, where V_{sh} is the shock velocity. We have assumed that the post-shock proton velocity distribution in the fluid frame can be described by a Maxwellian distribution function. The post-shock proton temperature is given by

$$T = \frac{3}{16} \frac{m_p}{k} V_{sh}^2 = \frac{1}{3} \frac{m_p}{k} v_0^2 , \tag{4}$$

so that $l^2 = 3/(2v_0^2)$. Here we have assumed that the shock is fast and that only protons are thermalized behind the shock (model A). If complete thermalization occurred behind the shock wave, assuming complete ionization and 10% He by number relative to H, we would have $l^2 = 2.46/v_0^2$ (model B). The function $\sigma_x(v)$ can be found from the work of McClure (1966); it is a very steep function of proton energy at high energies. The integral can be written as

$$\langle \sigma_x v \rangle_s = \frac{l^3}{\pi^{3/2}} \int_{-1}^{+1} \int_0^\infty v\sigma_x(v)[\exp(-l^2 v^2 - l^2 v_0^2 + 2vv_0\mu l^2)]v^2 dv 2\pi d\mu$$

$$= \left(\frac{3}{2\pi} \right)^{1/2} v_0 \int_0^\infty \sigma_x(y)\{\exp[-\tfrac{3}{2}(y-1)^2] - \exp[-\tfrac{3}{2}(y+1)^2]\}y^2 dy ,$$

where $y = v/v_0$. The results of carrying out this integral for a number of values of v_0 are shown in Figure 2. It has been assumed in this discussion that the incoming neutral fraction is not very large. If it were large, most of the low-velocity protons would undergo charge exchange and the proton velocity distribution would no longer be that used in equation (3).

The velocity distribution involved in $\langle \sigma_i v \rangle_f$ is quite complicated because it involves the velocity distribution of fast neutral particles. Fortunately, $\sigma_i(v)$ is not highly sensitive to velocity (Ptak and Stoner 1973), and we can approximate $\langle \sigma_i v \rangle_f$ by $\sigma_i(v_{th})v_{th}$, where v_{th} is the mean velocity of the fast particles. A typical value is $\sigma_i = 2.2 \times 10^{-16}$ cm^2.

In order to estimate the relative amounts of Hα emission in the broad and narrow components, there are two more factors that need to be taken into account. The first is that under the conditions present in Tycho's remnant, emission from fast atoms is optically thin in the Lyman lines (case A), while the emission from the slow atoms is
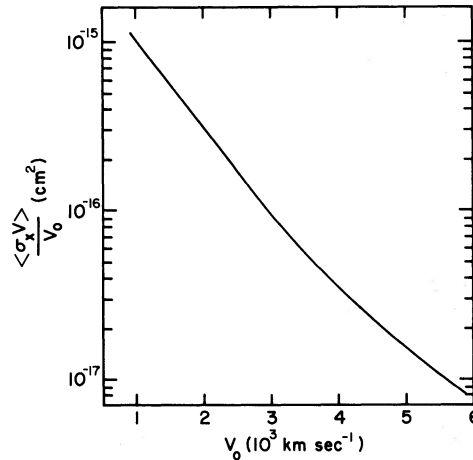
FIG. 2.—The quantity $\langle\sigma_x v\rangle/v_0$ as a function of v_0, the mean velocity of gas behind the shock wave. The quantity σ_x is the charge-exchange cross section, v is the relative velocity between the slow neutral atoms and the fast protons, and the brackets denote an average over the velocity distribution of the fast post-shock protons.

somewhat optically thick (see § IIIc). We estimate that this effect enhances the Hα emission from slow atoms by a factor of 6 relative to the emission from fast atoms. We note that this effect is decreased for the Hβ line so that the broad component should be relatively more important for Hβ.

The second effect is that hydrogen emission can occur as a result of charge exchange into an excited state. A quantitative analysis of this process is given by Bates and Dalgarno (1953). For the conditions in Tycho's remnant, the fraction of charge-exchange interactions that result in Hα emission, g_α, is 0.02–0.04. Charge exchange into an excited state is possible not only for a slow neutral atom interacting with a fast ion but also for a fast neutral atom interacting with a fast ion. In fact, a fast neutral atom undergoes $\langle\sigma_x v\rangle_f/\langle\sigma_i v\rangle_f$ exchanges before being ionized. The result of these effects is that

$$\frac{I(\text{broad})}{I(\text{narrow})} \approx \frac{\langle\sigma_x v\rangle_s}{6\langle\sigma_i v\rangle_f}\left[1 + g_\alpha\left(1 + \frac{\langle\sigma_x v\rangle_f}{\langle\sigma_i v\rangle_f}\right)\right], \tag{5}$$

where $I(\text{broad})$ and $I(\text{narrow})$ are the emission in the broad and narrow components, respectively.

The shock wave theory also leads to a prediction of the width of the broad emission component. The shape of the broad component spectrum depends on the orientation of the observation because of the anisotropic nature of the proton distribution function. The observations of Tycho's remnant indicate that a line of sight in the plane of the shock front should be considered. Using the coordinate system previously described, let the x-coordinate be along the line of sight. Then the emission rate as a function of velocity is given by

$$\phi(v_x) \propto \int\int_{-\infty}^{+\infty} v\sigma_x(v)\{\exp[-l^2(v^2 - 2v_0 v_z)]\}dv_y dv_z, \tag{6}$$

where it has been assumed that the initial neutral fraction is small and that the probability of H emission is independent of the proton velocity. We have calculated this integral for various values of v_0 and v_x in order to predict the FWHM of the emission as a function of v_0. Two models were considered: model A assumed $l^2 = 1.5/v_0^2$ (thermalization of protons), and model B assumed $l^2 = 2.46/v_0^2$ (thermalization of protons, He nuclei, and electrons). The results are shown in Figure 3. It can be seen that the FWHM levels out close to 4000 km s^{-1} for large values of v_0. This is because the FWHM velocity width of $\sigma_x(v)$ is approximately 4400 km s^{-1} (McClure 1966).

b) Tycho's Supernova Remnant

We now apply these considerations to Tycho's remnant. The distance to Tycho's remnant is not well determined. As noted by Kamper and van den Bergh (1978), the distance of 6 kpc based on H I absorption features in the radio spectrum (Goss, Schwarz, and Wesselius 1973; Williams 1973) is uncertain because of possible noncircular motions in the outer spiral arm, although Goss (1979) has recently maintained that the distance is at least 5 kpc. A distance of 7.2 kpc has been derived from the surface brightness–diameter (Σ-D) relation for supernova remnants (Clark and Caswell 1976). This value is not reliable because it is unlikely that the particle acceleration
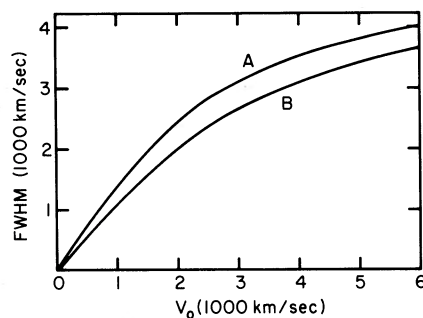
FIG. 3.—The full width at half maximum (FWHM) of the broad emission component as a function of v_0, the mean velocity of gas behind the shock wave, for the case of a shock wave viewed edge on. In model A, only protons are thermalized behind the shock wave; in model B, the gas consists of 10% He by number and is completely ionized and thermalized.

mechanism in Tycho's remnant is the same as that in the older remnants which are the calibrators for the Σ-D relation (Chevalier 1977). However, the proper motion of the filament that we observed is fairly well determined to be $0\rlap{.}''21$ yr^{-1} (Kamper and van den Bergh 1978). As the filament appears to be located at the outer edge of the radio remnant (Duin and Strom 1975), it is likely that we are observing a shock wave moving perpendicular to the line of sight. Once the shock velocity is determined, the distance to the remnant is determined.

The shock velocity can be found from the ratio I(broad)/I(narrow), which is observed to be in the range 0.4–1.3. The ratio is a sensitive function of v_0 because $\langle\sigma_x v\rangle_s$ is a strong function of v_0 (Fig. 2). The observed range corresponds to $v_0 = 1850 \pm 400$ km s^{-1}. In this estimate, we have neglected possible errors in the corrections for optical thickness and charge exchange to excited states. While these errors are quite uncertain, we expect that they are smaller than the error in the observed ratio I(broad)/I(narrow).

Another measure of the post-shock gas velocity is provided by the width of the broad emission component, which is observed to have a FWHM of 1800 ± 200 km s^{-1}. Taking into account the range of model A to model B in Figure 3, we deduce a value of $v_0 = 1600 \pm 400$ km s^{-1}. If there is complete thermalization in the shock wave, this range of shock velocity corresponds to a post-shock value of T_e between 3.5×10^7 and 9.8×10^7 K. The X-ray spectrum indicates that there is a component with an electron temperature of 4.1×10^7 K (Davison, Culhane, and Mitchell 1976). There may be complete thermalization in the shock wave, although partial thermalization is also possible. The value of v_0 deduced from the width is consistent with the value deduced from the ratio I(broad)/I(narrow). One assumption implicit in equation (6) is that the collisionless shock wave produces a Maxwellian distribution of protons. The observations appear to be consistent with this assumption.

Thus, both the ratio I(broad)/I(narrow) and the FWHM of the broad component indicate that $v_0 = 1700 \pm 400$ km s^{-1}. The shock velocity is 4/3 times v_0, and, combined with the observed proper motion of the filament, the distance to Tycho's remnant is 2.3 ± 0.5 kpc. At this distance, the average expansion velocity (radius divided by age) of Tycho's remnant is 6000 ± 1400 km s^{-1}. The average velocity should be less than the initial ejection velocity of the supernova shell because Tycho's remnant is in the blast wave stage of evolution and has been decelerating. Branch (1977) estimates that the initial expansion velocity of a Type I supernova is $10,900 \pm 700$ km s^{-1}, while Kirshner (1977) notes that there is evidence for the ejection of a shell at about 10,000 km s^{-1}. At a distance of 6 kpc, the average expansion velocity would be 15,600 km s^{-1}, which is inconsistent with observations of Type I supernovae. The average velocity at a distance of 2.3 ± 0.5 kpc is consistent with the observations.

Given the distance to Tycho's remnant, it is of interest to deduce the absolute magnitude of the supernova at maximum. As discussed in § II, there is some controversy over the apparent magnitude of Tycho's supernova at maximum light; we adopt m_v(max) $= -4.4 \pm 0.4$, taking into account Pskovskii's (1978) recent discussion. The absorption corrected magnitude is then m_v^0(max) $= -6.5 \pm 0.9$. At a distance of 2.3 ± 0.5 kpc, the absolute magnitude is M_v(max) $= -18.3 \pm 1.3$. Type I supernovae have $B - V \approx 0.15$ at maximum light and $m_{pg} = B - 0.32$ (Branch and Bettis 1978), so that M_{pg}(max) $= -18.8 \pm 1.3$. This maximum magnitude can be compared with the maximum magnitudes of extragalactic Type I supernovae. Tammann (1978) estimates that Type I supernovae in E and S0 galaxies have M_{pg}(max) $= -19.82 \pm 0.16$ with $\sigma = 0.42$. Type I supernovae in spiral galaxies appear to be somewhat fainter than those in E galaxies, but this may be due to absorption within the parent galaxy (Branch and Bettis 1978; Tammann 1978). We note that Tammann takes the Hubble constant, H_0, to be 50 km s^{-1} Mpc^{-1}; a larger value of H_0 could bring the magnitude of Tycho's supernova into better agreement with the value found for extragalactic supernovae. In any case the value of M_{pg}(max) for extragalactic supernovae is within the errors of the magnitude deduced for Tycho's supernova.

The new distance to Tycho's remnant changes some of the discussion of Kirshner and Chevalier (1978) and Chevalier and Raymond (1978), which was based on a distance of 6 kpc. We now take the distance to be 2.3 kpc. The ambient density, n_0, can again be deduced on the assumption that the high-temperature X-ray component is

produced by gas behind the blast wave. The luminosity of the post-shock gas is approximately (Gorenstein and Tucker 1976)

$$L(\Delta E) = 5 \times 10^{33} n_0^2 R_{\rm pc}^3 \text{ ergs s}^{-1},$$

where $R_{\rm pc}$ is the radius in parsecs. Taking the luminosity to be 5×10^{34} ergs s^{-1} (Davison, Culhane, and Mitchell 1976) yields $n_0 \approx 0.9$ H atoms cm^{-3}. Given the ambient density, the total energy, E_0, can be found from the Sedov (1959) blast wave relation

$$R = \left(\frac{2E_0}{\rho_0}\right)^{1/5} t^{2/5}.$$

The energy is deduced to be 1.3×10^{50} ergs. If the typical velocity of matter ejected in a Type I supernova is 10,000 km s^{-1}, this energy corresponds to an ejected mass of 0.13 $M_\odot$. This is much smaller than the swept-up mass of 1.7 $M_\odot$ and is consistent with Tycho's remnant being in the blast wave stage of evolution. The total number of particles that the remnant has interacted with is a factor of 4 smaller than the estimate of CR which was based on a distance of 6 kpc. This reduces the upper limit on the ionizing energy emitted by the supernova to about 1×10^{47} ergs, although there is still considerable uncertainty in this estimate.

Finally, we consider the surface brightness of the filaments. Using the formula given by CR, the predicted surface brightness of Hα is $3.0 \times 10^{-5} \alpha (1 - x)$ ergs cm^{-2} s^{-1} sr^{-1}, where α is a term to take into account the orientation of the shock front and is equal to unity if the shock front is viewed face-on. As noted by CR, α can reach values greater than 10. The observed value of the surface brightness is 7×10^{-5} ergs cm^{-2} s^{-1} sr^{-1} using the observed flux from Table 2 and assuming that the emission is uniformly distributed over the aperture.

Tycho's remnant is probably not well into the blast wave stage of evolution. If the dependence of radius on time is written as $R \propto t^s$, the calculations of Rosenberg and Scheuer (1973) show that the ratio of swept-up mass to ejected mass must be about 15 in order to have $s = 0.4$. At the stage of evolution of Tycho's remnant, s may be about 0.5 or 0.6, although there is considerable uncertainty in this estimate. The observations of the filaments in Tycho's remnant (Kamper and van den Bergh 1978) show that $s = 0.38 \pm 0.01$. The velocity of the shock wave is proportional to s, indicating that some deceleration may have occurred in the regions of optical emission. If the post-shock pressure is approximately constant around the remnant, the shock velocity is proportional to the square root of the preshock density. A density increase of a factor of 2 would be sufficient to give the observed possible deceleration. This density change cannot account for the variation in the surface brightness of the emission around the remnant. This must be due either to variations in the neutral fraction of the preshock gas or to variations in the geometry of the emitting region.

c) The Balmer Decrement

The Hα/Hβ ratio found in the emission from Tycho's remnant is in the range 3.5–5.0 (see § II). Schweizer and Lasker (1978) also find a large Balmer decrement in the remnant of SN 1006; they estimate $I(\text{H}\alpha)/I(\text{H}\beta) \approx 5.7$, although the uncertainty is large. The theoretical predictions given by CR were either for case A (optically thin in the Lyman lines) or case B (optically thick in the Lyman lines). In these two limits, for case A $I(\text{H}\alpha)/I(\text{H}\beta) = 3.0$, and for case B $I(\text{H}\alpha)/I(\text{H}\beta) = 3.6$.

However, it is not clear that either case A or case B strictly applies. The optical depth in the Lyman lines can be estimated from the column density of neutral hydrogen. Let n_0 be the total hydrogen density at the shock wave, so that $(1 - x)n_0$ is the neutral hydrogen density where x is the ionization fraction. If the initial neutral fraction is small, the neutral density behind the shock declines exponentially, with the scale length l determined by the ionization of the hydrogen atoms. Thus

$$l \approx \frac{v_{\rm sh}}{(\langle \sigma_{ie} v \rangle + \langle \sigma_{ip} v \rangle) 4 x n_0} \tag{7}$$

where $v_{\rm sh}$ is the shock velocity, v is the relative velocity between the hydrogen atom and an ionizing particle, σ_{ie} is the cross section for ionization by electrons, σ_{ip} is the cross section for ionization by protons, and the angular brackets indicate an average over the velocity distributions of the neutral and the ionizing particles. The factor of 4 in the denominator is based on the compression which occurs in a strong adiabatic shock. The ionization cross sections (e.g., Ptak and Stoner 1973) are not highly velocity-dependent for the velocity range relevant to Tycho's remnant, and l is approximately given by $1 \times 10^{15}/x n_0$ cm, where n_0 is in H atoms cm^{-3}. The optical depth in the post-shock gas is given by

$$\tau = \int n(\text{H I}) \sigma dz = (1 - x) n_0 \sigma l, \tag{8}$$

where z is a coordinate perpendicular to the shock front and σ is the cross section at the frequency in question.

The effective optical depth in a line can be estimated by $1/e$ times the line-center optical depth (cf. MacAlpine 1976). Thus, σ is $1/e$ times the cross section at line center. For $L\beta$ we have

$$\sigma = 3.5 \times 10^{-15} T_4^{-1/2} \text{ cm}^2 , \tag{9}$$

and for $L\gamma$ we have

$$\sigma = 1.2 \times 10^{-15} T_4^{-1/2} \text{ cm}^2 , \tag{10}$$

where T_4 is the gas temperature in units of 10^4 K. These cross sections lead to the following optical depths:

$$\tau(L\beta) \approx 4.0 \frac{(1 - x)\delta}{x} T_4^{-1/2} , \tag{11}$$

$$\tau(L\gamma) \approx 1.4 \frac{(1 - x)\delta}{x} T_4^{-1/2} , \tag{12}$$

where δ is the fraction of the neutral gas that is at the temperature under consideration. As discussed in § IIIa, it is expected that there are two temperature components for the post-shock neutral gas. In Tycho's remnant, the cool component may have $\delta \approx 0.3$. The larger number of scatterings of $L\beta$ than of $L\gamma$ results in a more complete conversion of $L\beta$ to $H\alpha$ than of $L\gamma$ to $H\beta$ and thus enhances the intensity of $H\alpha$ over $H\beta$.

In order to examine the effect quantitatively, we consider two models. In model 1, the neutral density ahead of the shock is assumed to be $(1 - x)n_0$; and in model 2, it is assumed to be 0. Model 1 should apply to the narrow component for a shock in a homogeneous medium while model 2 should apply to the broad wings (see § IIIa) or to a shock in a small cloud. Let i and j refer to two layers of gas. The fraction of photons emitted by layer i which escape is $E_2(\tau_i)/2$ for model 1 and is $E_2(\tau_i)/2 + E_2(\tau - \tau_i)/2$ for model 2, where E_2 is the exponential integral of index 2. The fraction of the photons emitted by layer i that are absorbed by layer j is proportional to min $[3, E_1(|\tau_i - \tau_j|)]n(\text{H I})_j$. The cutoff value of 3 corresponds to infinite planar geometry (Shull and McKee 1979). The absorbed radiation is multiplied by the branching ratios for $L\beta$ and $L\gamma$ (Wiese, Smith, and Glennon 1966) and is used as the emitted radiation for the next iteration. In calculating the emission, the $n = 3$ excitation cross sections are from Kingston and Lauer (1966); for $n = 4$, these are scaled by the oscillator strength divided by the threshold energy. It is assumed that excitation and ionization are by electrons with a temperature of 3×10^7 K. Protons would give a slightly lower $I(\text{H}\alpha)$ and a similar $I(\text{H}\alpha)/I(\text{H}\beta)$ ratio.

Figure 4 shows the number of $H\alpha$ photons produced per ionization as a function of $\tau(L\beta)$ for models 1 and 2. It can be seen that for model 1, $I(\text{H}\alpha)$ does not approach case A as $\tau \to 0$. This is because half of the $L\beta$ photons go into the preshock gas and about half of these are converted to $H\alpha$. The predicted number of $H\alpha$ photons per ionization is somewhat different from the results presented in Chevalier and Raymond (1978) because different atomic data have been used in the calculations.

The $I(\text{H}\alpha)/I(\text{H}\beta)$ ratio as a function of $\tau(L\beta)$ is given in Figure 5. It can be seen that over the range in $\tau(L\beta)$ that is thought to occur in Tycho's remnant, values of $I(\text{H}\alpha)/I(\text{H}\beta)$ in the range 4–5 are quite plausible. However, there are inaccuracies in the calculation. The assumption that the neutral density is proportional to $\exp(-z/l)$
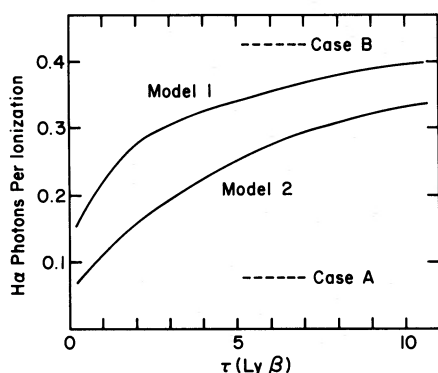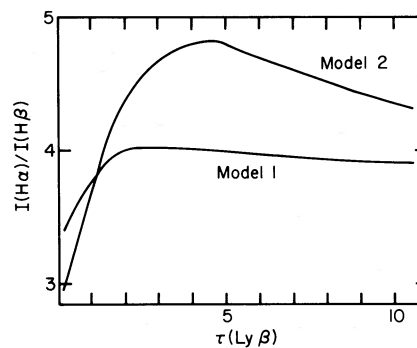

FIG. 4.—The number of $H\alpha$ photons produced per ionization in the post-shock gas as a function of the optical depth in the $L\beta$ line. Case A would apply if the gas were optically thin in the Lyman lines, and case B would apply if it were optically thick in the Lyman lines. In model 1, the gas ahead of the shock has a constant neutral fraction and density, and in model 2, the preshock gas has no neutral atoms.

FIG. 5.—The ratio of the intensity of $H\alpha$ and $H\beta$ lines as a function of optical depth in the $L\beta$ line. The two models are described in the legend to Fig. 4.

is only good provided that the neutral fraction is small. The observations select out the brightest filaments, and these may well have a large neutral fraction. These calculations demonstrate that $I(H\alpha)/I(H\beta)$ should be greater than 3 for the narrow component, but they are not accurate enough for inference of shock parameters from an observed $I(H\alpha)/I(H\beta)$ ratio.

A similar situation holds for the $I(H\alpha)/I(H\gamma)$ ratio. The observed value of 13 in Tycho's remnant is larger than the values of 7.5 (case A) and 9.0 (case B) given in CR. An approximate radiative transfer calculation shows that the $I(H\alpha)/I(H\gamma)$ ratio can be close to 15 for model 2 with $\tau(L\beta) \approx 5$.

IV. APPLICATION TO OTHER REMNANTS

a) SN 1006

As mentioned by CR, the observations of the remnant of SN 1006 (Schweizer and Lasker 1978) can be explained by the theory discussed here. Although there are fewer data on this remnant than on Tycho's remnant, it has been detected as an X-ray source. Winkler and Laird (1976) find that the characteristic X-ray temperature is about 4 keV. If there is complete thermalization in the shock wave, the shock velocity is 1800 km s^{-1}, corresponding to $v_0 = 1350$ km s^{-1}. The shock velocity could be higher if there is incomplete thermalization, as appears to be the case in Tycho's remnant. A much higher shock velocity is unlikely because the SN 1006 remnant is older than Tycho's remnant. We predict that there should be a broad emission component in the spectrum of the SN 1006 remnant with an intensity comparable to that in the narrow component (to within a factor of 3).

b) The Cygnus Loop

The high-velocity Hα features observed by Kirshner and Taylor (1976) in the Cygnus Loop may also be due to the type of shock emission described here. A competing model for this emission is the accelerated cloudlet model of McKee, Cowie, and Ostriker (1978). One difference between the models is the predicted column density of neutral hydrogen. In the model of McKee, Cowie, and Ostriker (1978), it is about 10^{19} cm^{-2}, while in the present model it is orders of magnitude smaller (see § IIIc). Giovanelli and Haynes (1979) have searched for high-velocity 21 cm emission in the places observed by Kirshner and Taylor and have failed to find any with a sensitivity level of 10^{19} cm^{-2}. This gives weak evidence against the model of McKee et al.

Another difference between the models may be in the width of the high-velocity feature. In the shock model, the shock velocity in the Cygnus Loop is such that charge exchange dominates ionization. The observations refer to the central region of the Cygnus Loop so that the velocity distribution of fast neutrals is given by

$$\phi(v_z) \propto \int\int_{-\infty}^{\infty} v\sigma_x(v) \exp\left[-l^2(v_0{}^2 - 2v_0 v_z)\right]dv_x dv_y ,$$

where l and the coordinate system are as defined in equation (3). At the velocities of several 100 km s^{-1} present in the Cygnus Loop, complete thermalization may occur behind the shock front, and we take $l^2 = 2.46/v_0{}^2$ (see § IIIa). Under these circumstances, the Gaussian width of the line is approximately $0.45v_0$ and the maximum emission in the line is at v_0. The highest LSR velocity found by Kirshner and Taylor (1976) for the line center is 267 km s^{-1}. Assuming that this is the value of v_0, the predicted Gaussian width is 120 km s^{-1}. Of the five observed high-velocity features, three of them have widths in the range 91–93 km s^{-1}, which is in fair agreement with the predicted value. McKee et al. do not discuss the line width predicted by their model, but it is probably small unless the cloudlets are in the process of being disrupted or a distribution of cloudlets is observed.

One problem with the shock theory is that the predicted surface brightness is somewhat lower than that observed. For $v_0 = 267$ km s^{-1} and $n_0 = 0.25$ cm^{-3} (Rappaport et al. 1974), the predicted intensity is

$$\epsilon_{0.1}\alpha(1 - x)2.2 \times 10^{-7} \text{ ergs cm}^{-2} \text{ s}^{-1} \text{ sr}^{-1} ,$$

where $\epsilon_{0.1}$ is the number of Hα photons emitted per ionization in units of 0.1. The quantity α must be close to unity if the shock wave is observed face-on. The observed regions have surface brightnesses in the range 6×10^{-7} to 3×10^{-6} ergs cm^{-2} s^{-1} sr^{-1}. It is clear that the neutral fraction of the preshock gas must be large for the theory to apply.

The major difference between the two models for the Cygnus Loop emission is in the strength of the forbidden lines of O^0, O^+, O^{++}, N^+, etc. In the shock model, they are predicted to be very faint.

c) The η Carinae Region

A nonthermal radio source, G287.8−0.5, was found by Jones (1973) in low-frequency observations of the η Carinae region. Elliott (1979) has recently found evidence for high-velocity motions in this region which he attributes to a supernova remnant associated with the radio source. The positional accuracy of the radio source is not high enough to be definite on this point.

Elliott found that there is a broad component to the Hα emission with a FWHM of 655 km s^{-1}; the broad component is absent in the emission of [N II] and [S II]. The broad emission is fairly symmetrically centered on zero velocity, indicating that, if the shock wave theory applies, Elliott must have observed the shock front nearly edge-on. Thus, using Figure 3, we deduce that the adiabatic shock wave has $v_0 \approx 600$ km s^{-1}, corresponding to a shock velocity of 800 km s^{-1}. At this velocity, charge exchange is far more likely than ionization in the post-shock region, and essentially all of the shock emission should be in the broad component. The narrow Hα component observed by Elliott, as well as the [N II] and [S II] emission, must be due to some other source.

Considering the symmetric nature of the broad line profile, one possibility is that the emission is not from a shock wave. The emission mechanism described here will operate in any situation where a partially neutral gas is heated on a time scale that is short compared to the ionization time scale. There is diffuse X-ray emission from the η Carinae region (Seward *et al.* 1979), but the heating source for the gas is not known.

V. SUMMARY AND DISCUSSION

The emission mechanism described in this paper shows that it is possible to observe optical emission from strong adiabatic shock waves. Previously, it had been assumed that these shock waves could only be observed by their X-ray radiation, although Cowie *et al.* (1979) have recently shown that the shock waves might be observable in ultraviolet hydrogen absorption lines. The observations of Tycho's remnant can be compared in detail with the predictions of the shock wave theory. The ratio of the broad to narrow emission components is very sensitive to the shock velocity. Our observations of the Hα line profile in Tycho's remnant, when combined with the shock theory and the proper-motion observations of Kamper and van den Bergh (1978), yield a distance of 2.3 $\pm$ 0.5 kpc. If the shock theory is applicable, this may be the most reliable distance determination to Tycho's supernova.

The structure of high-velocity shock waves, such as that in Tycho's remnant, is poorly understood. The high Mach number and low density are in a regime that is not accessible in the laboratory. Yet, such high-velocity shocks can occur in a number of astronomical situations—for example, the accretion of gas onto compact objects. The observation of fast shock waves in emission nebulae like Tycho's remnant may give more information on the structure of these shock waves.

REFERENCES

Baade, W. 1945, *Ap. J.*, **102**, 309.
Barbon, R., Ciatti, F., and Rosino, L. 1973, *Astr. Ap.*, **25**, 241.
Bates, D. R., and Dalgarno, A. 1953, *Proc. Phys. Soc. London A*, **66**, 972.
Branch, D. 1977, *M.N.R.A.S.*, **179**, 401.
Branch, D., and Bettis, C. 1978, *A.J.*, **83**, 224.
Brodskaya, E. S., and Grigor'eva, N. B. 1962, *Astr. Zh.*, **39**, 754 (English transl. in *Soviet Astr.—AJ.*, **6**, 586).
Chevalier, R. A. 1977, *Ann. Rev. Astr. Ap.*, **15**, 175.
Chevalier, R. A., and Raymond, J. C. 1978, *Ap. J. (Letters)*, **225**, L27 (CR).
Clark, D. H., and Caswell, J. L. 1976, *M.N.R.A.S.*, **174**, 267.
Cowie, L., Laurent, C., Vidal-Madjar, A., and York, D. G. 1976, *Ap. J. (Letters)*, **229**, L81.
Davison, P. J. N., Culhane, J. L., and Mitchell, R. J. 1976, *Ap. J. (Letters)*, **206**, L37.
Duin, R. M., and Strom, R. G. 1975, *Astr. Ap.*, **39**, 33.
Elliott, K. H. 1979, *M.N.R.A.S.*, **186**, 9P.
Giovanelli, R., and Haynes, M. P. 1979, *Ap. J.*, **230**, 404.
Gorenstein, P., and Tucker, W. H. 1976, *Ann. Rev. Astr. Ap.*, **14**, 373.
Goss, W. M. 1979, private communication.
Goss, W. M., Schwarz, U. J., and Wesselius, P. R. 1973, *Astr. Ap.*, **28**, 305.
Jones, B. B. 1973, *Australian J. Phys.*, **26**, 545.
Kamper, K. W., and van den Bergh, S. 1978, *Ap. J.*, **224**, 851.
Kingston, A. E., and Lauer, J. E. 1966, *Proc. Phys. Soc.*, **88**, 597.
Kirshner, R. P. 1977, *Ann. NY Acad. Sci.*, **302**, 81.

Kirshner, R. P., and Chevalier, R. A. 1978, *Astr. Ap.*, **67**, 267.
Kirshner, R. P., and Taylor, K. 1976, *Ap. J. (Letters)*, **208**, L83.
MacAlpine, G. M. 1976, *Ap. J.*, **204**, 694.
McClure, G. W. 1966, *Phys. Rev.*, **148**, 47.
McKee, C. F., Cowie, L. L., and Ostriker, J. P. 1978, *Ap. J. (Letters)*, **219**, L23.
Miller, J. S., and Mathews, W. G. 1972, *Ap. J.*, **172**, 593.
Minkowski, R. 1964, *Ann. Rev. Astr. Ap.*, **2**, 247.
Pskovskii, Yu. P. 1978, *Astr. Zh.*, **55**, 737 (*Soviet Astr.—AJ.*, **22**, 420).
Ptak, R., and Stoner, R. E. 1973, *Ap. J.*, **185**, 121.
Rappaport, S., Doxsey, R., Solinger, A., and Borken, R. 1974, *Ap. J.*, **194**, 329.
Rosenberg, I., and Scheuer, P. A. G. 1973, *M.N.R.A.S.*, **161**, 27.
Schweizer, F., and Lasker, B. M. 1978, *Ap. J.*, **226**, 167.
Sedov, L. I. 1959, *Similarity and Dimensional Methods in Mechanics* (New York: Academic Press).
Seward, F., Forman, W., Giacconi, R., Jones, C., and Pye, J. 1979, *Bull. A.P.S.*, **24**, 641.
Shull, J. M., and McKee, C. F. 1979, *Ap. J.*, **227**, 131.
Tammann, G. A. 1978, *Mem. Soc. Astr. Italiana*, **49**, 315.
van den Bergh, S. 1970, *Nature*, **225**, 503.
Whitford, A. E. 1958, *A.J.*, **63**, 201.
Wiese, W. L., Smith, M. W., and Glennon, B. M. 1966, *Atomic Transition Probabilities* (Washington: National Bureau of Standards).
Williams, D. R. W. 1973, *Astr. Ap.*, **28**, 309.
Winkler, P. F., and Laird, F. N. 1976, *Ap. J. (Letters)*, **204**, L111.

Roger A. Chevalier: Department of Astronomy, University of Virginia, P.O. Box 3818, Charlottesville, VA 22903

Robert P. Kirshner: Department of Astronomy, University of Michigan, Ann Arbor, MI 48109

John C. Raymond: Harvard-Smithsonian Center for Astrophysics, 60 Garden Street, Cambridge, MA 02138